

# PERFORMANCE ANALYSIS IN D2D PARTIAL NOMA-ASSISTED BACKSCATTER COMMUNICATION

Thu-Ha Thi Pham<sup>1</sup> , Nhat-Truong Thanh Nguyen<sup>2</sup>, Quoc-Su Nguyen<sup>3</sup>, Thanh Hon Nguyen<sup>4</sup>, Bui Vu Minh<sup>5</sup> , Quang-Sang Nguyen<sup>6,\*</sup> , Minh Tran<sup>7</sup> 

<sup>1</sup>Faculty of Electrical and Electronics Engineering, Ton Duc Thang University, Ho Chi Minh City 70000, Vietnam.

<sup>2</sup>Ho Chi Minh City Technical-Economic College (HOTEC), Faculty of Electrical Engineering, Ho Chi Minh City 70000, Vietnam.

<sup>3</sup>Faculty of Information Technology, Ho Chi Minh City University of Industry and Trade, Ho Chi Minh City 70000, Vietnam.

<sup>4</sup>Vietnam Posts and Telecommunications Group-Ho Chi Minh City Telecommunications, Vietnam.

<sup>5</sup>Faculty of Engineering and Technology, Nguyen Tat Thanh University, 300A-Nguyen Tat Thanh, Ward 13, District 4, Ho Chi Minh City 754000, Vietnam.

<sup>6</sup>Posts and Telecommunications Institute of Technology, Ho Chi Minh City, Vietnam.

<sup>7</sup>Advanced Intelligent Technology Research Group, Faculty of Electrical and Electronics Engineering, Ton Duc Thang University, Ho Chi Minh City 70000, Vietnam.

42101299@student.tdtu.edu.vn, nguyenthannhattruong@hotec.edu.vn, sunq@huit.edu.vn, honnt.hcm@vnpt.vn, bvminh@ntt.edu.vn, sangnq@ptit.edu.vn, tranhoangquangminh@tdtu.edu.vn

\*Corresponding author: Quang-Sang Nguyen; sangnq@ptit.edu.vn

DOI: 10.15598/aeec.v23ix.250314

Article history: Received Mar 07, 2025; Revised Apr 09, 2025; Accepted Apr 14, 2025; First Published Apr 27, 2025.

This is an open access article under the BY-CC license.

**Abstract.** Backscatter communication (BackCom) is an emerging technology that enables ultra-low-power wireless transmission by reflecting ambient signals. To enhance spectral efficiency and improve communication performance, we integrate BackCom with partial non-orthogonal multiple access (NOMA). In this paper, we propose a partial NOMA-assisted backscatter communication system for device-to-device (D2D) networks, where a backscatter device (BD) reflects signals from a source to two users via distinct channels. We derive closed-form expressions for the outage probability (OP) of both users under Rayleigh fading and various decoding conditions. The analytical results provide insights into the impact of key system parameters, such as the reflection coefficient, power allocation factors, and channel conditions, on the system's reliability. In particular, by adjusting the bandwidth allocation coefficient, we are able to compare the system performance between partial NOMA and full NOMA schemes. The findings of this study offer valuable guidance for the de-

sign of energy-efficient and spectrally efficient wireless networks utilizing BackCom and NOMA.

## Keywords

**Backscatter Communication, Partial NOMA, Outage Probability, Device-to-Device, Power Allocation.**

## 1. Introduction

As wireless communication evolves towards 5G, 6G, and beyond, the demand for high spectral efficiency, low-latency, and massive connectivity continues to rise. In this context, Non-Orthogonal Multiple Access (NOMA) has emerged as a key multiple access technique capable of significantly enhancing network capacity by enabling multiple users to share the same

frequency and time resources. Compared to traditional Orthogonal Multiple Access (OMA) schemes, NOMA improves spectral efficiency, supports massive connectivity, and enhances fairness by employing power-domain or code-domain multiplexing. Given its potential, NOMA has been extensively studied in various wireless network architectures, including Reconfigurable Intelligent Surfaces (RIS), BackCom, and cognitive radio networks [1, 2]. However, challenges such as interference management, energy efficiency, security, and optimal resource allocation remain key concerns, requiring innovative solutions to unlock the full potential of NOMA in future wireless networks. In hybrid satellite-terrestrial relay systems, NOMA has demonstrated its potential to improve communication efficiency, particularly when combined with mmWave technology, leading to enhanced spectral utilization and improved system capacity [3]. Additionally, full-duplex multi-hop NOMA systems have been analyzed under practical impairments such as imperfect interference cancellation and near-field path loss, providing insights into their performance limits and reliability [4]. In the realm of 5G and 6G, efficient spectrum sharing and resource allocation are critical for managing the increasing network load. Several studies have investigated spectrum-sharing models and their impact on NOMA-based systems. Papers [1, 2] provide a comprehensive survey of advanced techniques for spectrum sharing in 5G, analyzing challenges such as interference, power allocation, and user fairness. Moreover, paper [5] discusses AI-driven spectrum management, where machine learning models can optimize resource allocation in NOMA-enabled networks. Papers [6, 7] delve into the integration of cognitive radio (CR) with NOMA, presenting dynamic spectrum access techniques that enhance spectral efficiency in highly congested environments. Furthermore, resource allocation strategies for uplink NOMA in hybrid spectrum access for 6G-enabled cognitive IoT have been proposed, ensuring optimal spectrum utilization and minimizing interference in dense network scenarios [8]. Paper [9] examines uplink resource allocation in 5G systems, while papers [10, 11] investigate the ergodic capacity and MIMO techniques in NOMA networks, demonstrating how multiple antennas can enhance system performance. These studies highlight the importance of intelligent spectrum utilization in ensuring seamless 5G and 6G network operations. Recent studies have proposed various approaches to enhance the performance of NOMA in different scenarios. For instance, employing multiple Aerial Intelligent Reflecting Surfaces (Aerial IRSs) has been shown to improve system capacity by optimizing their positions and reflection angles, thereby enhancing signal quality and reducing interference in NOMA networks [12]. Additionally, a comparison between MIMO-NOMA and MIMO-OMA in clustered multi-user scenarios indi-

cates that MIMO-NOMA can achieve higher capacity, particularly when effective power allocation strategies and beamforming techniques are applied [13].

Beyond spectrum allocation, performance optimization in NOMA is a major research area that addresses issues such as OP, power efficiency, and transmission reliability. Paper [14] introduces a power beacon-assisted symbiotic radio network, analyzing its outage performance and energy harvesting efficiency. Paper [15] explores the integration of active reconfigurable repeaters in NOMA-based IoT networks, improving signal strength, security, and covertness. Similarly, paper [16] proposes a hybrid active-passive STAR-RIS-based NOMA system, investigating energy-rate trade-offs and rate adaptation techniques to maximize spectral efficiency. Meanwhile, paper [17] studies a dual-hop mixed RF-FSO system combined with NOMA, assessing the impact of atmospheric turbulence and fading conditions on transmission performance. Extending this work, paper [18] evaluates the ergodic rate and effective capacity of RIS-assisted NOMA networks under Nakagami-m fading environments. Additionally, large-scale heterogeneous networks employing NOMA have been studied, revealing significant improvements in spectrum efficiency and network capacity compared to conventional access techniques [19]. Likewise, power allocation strategies for cognitive radio networks using NOMA have been explored, demonstrating their effectiveness in optimizing spectral efficiency while ensuring fair resource distribution [20].

A key technological enabler for NOMA enhancement is RIS, which can dynamically manipulate the wireless environment to improve signal propagation. Paper [21] investigates how RIS can enhance data rates and energy efficiency in millimeter-wave (mmWave) NOMA systems, addressing high-frequency signal attenuation. Paper [22] examines holographic RIS for downlink NOMA in IoT networks, focusing on short-packet communication and latency reduction. Additionally, paper [23] analyzes physical layer security in RIS-aided NOMA networks, evaluating secrecy OP in the presence of non-colluding eavesdroppers. Paper [24] explores the potential of RIS-assisted ambient BackCom, highlighting its capability to improve energy efficiency while maintaining robust data transmission. Further, paper [25] employs deep learning techniques to optimize RIS-assisted cooperative NOMA-IoT networks, demonstrating how AI-driven methods can enhance power control and interference mitigation. Security and reliability are paramount concerns in NOMA-based networks, given their susceptibility to eavesdropping, jamming, and interference. Paper [26] examines the security-reliability trade-off in SWIPT-enabled full-duplex relaying for NOMA, revealing critical insights into interference and power transfer effects. Paper [27] studies the impact of I/Q imbalance

on security and reliability in CR-NOMA IoT networks, proposing countermeasures for mitigating transceiver imperfections. Papers [28,29] focus on securing massive MIMO-NOMA networks using ZF beamforming and artificial noise, demonstrating how these techniques can enhance secrecy capacity. Meanwhile, paper [30] investigates artificial noise-based security mechanisms for downlink massive MIMO-NOMA systems, providing strategies to mitigate potential attacks. Papers [31, 32] explore cooperative relay selection strategies for secure NOMA, proposing optimized relay deployment techniques to balance security and system reliability. Moreover, a general MIMO framework for both uplink and downlink NOMA transmission has been proposed using signal alignment, which helps mitigate interference and improve overall system robustness [33]. The advent of Artificial Intelligence (AI) and Machine Learning (ML) in NOMA has further accelerated advancements in power allocation, interference management, and dynamic spectrum access. Paper [34] presents a dynamic LSTM-based spectrum-sharing model, demonstrating how deep learning can improve adaptive resource allocation in NOMA-based CP-OFDMA networks. Similarly, paper [35] investigates ML-based power allocation strategies that maximize sum-rate and fairness, proving that AI-driven algorithms can outperform traditional heuristic-based approaches. Papers [5, 25] highlight AI's role in optimizing NOMA-IoT networks, showcasing how reinforcement learning and deep learning models can adaptively enhance system performance. These studies underscore the potential of AI-driven resource management in next-generation NOMA networks. Additionally, cooperative NOMA has been examined in the context of 5G systems, where cooperative relaying strategies can enhance communication reliability and system efficiency [36]. Cooperative NOMA has also been studied alongside simultaneous wireless information and power transfer (SWIPT), demonstrating its potential to support energy-constrained networks while improving transmission performance [37].

In addition to RIS and AI-driven optimizations, ambient BackCom has emerged as a promising solution for energy-efficient NOMA systems, particularly in low-power IoT applications. Paper [38] introduces wireless-powered NOMA communication leveraging ambient backscatter, demonstrating significant energy savings. Paper [39] extends this approach by incorporating relay cooperation, enhancing backscatter transmission efficiency. Paper [40] investigates wireless-powered relaying with ambient backscatter, proving its feasibility for ultra-low-energy communication networks. Several studies analyze the performance of ambient backscatter systems under different channel conditions. Papers [41, 42] model the performance of wireless networks incorporating backscatter devices, evaluating their impact on OP and reliability. Papers [43–47]

explore real-world applications of backscatter-assisted NOMA in IoT, agriculture, and large-scale multi-tag systems, proving its adaptability to diverse environments. Furthermore, cooperative full-duplex relaying has been studied for downlink NOMA systems, offering significant improvements in performance through optimized power allocation and interference management [48]. In the context of low-cost BackCom applications, studies have demonstrated its feasibility for agricultural use, showcasing an energy-efficient communication model tailored for smart farming [46]. From a security perspective, BackCom also faces challenges related to eavesdropping and interference. Paper [49] proposes randomized continuous wave techniques for enhancing the security of backscatter-based transmissions, while paper [50] studies multi-tag backscatter security strategies for mitigating interception threats. Lastly, paper [51] compares jamming and cooperative methods for securing multi-tag ambient BackComs, presenting innovative strategies to enhance system robustness against malicious attacks.

In recent years, the integration of BackCom with NOMA has gained significant attention due to its potential to enhance spectral and energy efficiency in wireless communication systems. Various studies have explored different approaches to optimizing such systems, particularly in terms of OP and energy efficiency. Among them, several works have investigated RIS to enhance BackCom-based NOMA networks, such as the study on RIS-assisted ambient BackCom systems, which analyzes OP and key performance trade-offs [24]. However, unlike this work, our model does not rely on RIS but instead focuses on partial NOMA, where resource allocation and user pairing strategies play a crucial role in performance enhancement. Similarly, uplink and downlink energy harvesting NOMA systems have been studied, where performance analysis has been conducted to assess OP and energy efficiency in such networks [52]. While these models provide useful insights into energy harvesting mechanisms, our study differentiates itself by incorporating BD that passively harvest energy from existing signals, reducing infrastructure complexity and enhancing system sustainability. Another significant research direction has been cooperative ambient backscatter systems, which focus on leveraging symbiotic radio to improve passive IoT communications through cooperation between devices [44]. However, these studies mainly emphasize cooperative transmission techniques rather than NOMA-based user access strategies, which are central to our model. Furthermore, works such as outage analysis for ambient BackCom systems provide detailed insights into fading channels and energy reflection mechanisms, which align with our OP analysis [45]. Nevertheless, our study extends beyond these contributions by integrating partial NOMA, which improves the transmission efficiency among multiple users

with minimal power consumption. Additionally, other works have explored wireless-powered D2D communications with ambient backscatter, where devices communicate without requiring a dedicated power source, optimizing performance in energy-constrained environments [49]. While this approach is beneficial for low-power applications, it does not incorporate NOMA-based user scheduling, which our model explicitly addresses. Several recent studies have investigated the integration of full NOMA with backscatter communication to improve spectrum and energy efficiency. For instance, in [43], a full NOMA-enhanced backscatter system is proposed, where the backscatter device reflects superimposed signals to multiple users across the entire spectrum. While this approach maximizes spectral efficiency, it leads to significant inter-user interference and increased SIC complexity, especially for the weak user. Similarly, the study in [59] applies full NOMA with optimized resource allocation, but it relies heavily on accurate CSI, which may not be practical in low-power IoT scenarios. Another work, [60], proposes a hybrid cellular-IoT framework using full NOMA, achieving high throughput but suffering from degraded performance at cell-edge users under imperfect decoding. By contrast, in this paper, our primary motivation is to address the challenges of spectral and energy efficiency in D2D communications, particularly for low-power IoT applications. BackCom is a promising solution for enabling ultra-low-power transmissions, but it typically suffers from low data rates and limited coverage due to its passive nature. On the other hand, NOMA techniques can significantly improve spectral efficiency and support massive connectivity. However, conventional full NOMA schemes introduce strong inter-user interference and decoding complexity, which are not ideal for energy-constrained or passive systems. Unlike the aforementioned full NOMA schemes, our approach is especially suitable for energy-constrained, low-complexity IoT applications. To overcome these limitations, we propose a partial NOMA-assisted backscatter system, which flexibly divides the transmission resources between dedicated and shared regions. This design allows us to reduce decoding complexity, enhance the reliability of the weak user, and balance spectral efficiency with energy constraints. By integrating partial NOMA with BackCom, our study provides a novel resource allocation framework that enhances spectral efficiency while maintaining low power consumption. The main contributions and novelties are listed as follows:

- We propose a novel system that combines backscatter communication (BackCom) with partial non-orthogonal multiple access (NOMA) to enhance spectral and energy efficiency. The backscatter device (BD) passively reflects signals from the source to multiple users, enabling

ultra-low-power communication while leveraging NOMA to improve user fairness and resource utilization.

- We derive analytical closed-form expressions for the OP of the proposed partial NOMA backscatter-assisted system under different decoding conditions. These expressions provide valuable insights into how key system parameters such as power allocation factors, reflection coefficients, and channel conditions affect overall system performance. In particular, by adjusting the bandwidth allocation coefficient, we are able to compare the system performance between partial NOMA and full NOMA schemes.
- We conduct Monte Carlo simulations to validate the theoretical OP analysis and assess system performance under various parameter settings. The results demonstrate that our proposed system outperforms conventional NOMA and BackCom schemes, offering improved reliability and efficiency.

## 2. System model

The figure 1 illustrates a Backscatter Device (BD)-assisted communication model, where a source (S) transmits signals to a Backscatter Device (BD), which then forwards the signals to two users, a near device ( $U_1$ ) and a distant device ( $U_2$ ). Acting as an intermediary node, the BD utilizes ambient backscatter communication to relay information while consuming minimal energy. The transmission process follows a two-step approach: the source first sends signals to the BD, which then reflects and transmits them to the users. This model is particularly beneficial for energy-efficient IoT networks and other low-power wireless communication applications. The second part of the figure presents the Partial NOMA transmission scheme, demonstrating how bandwidth is allocated among users. The transmission process is divided into two regions: Region-1 ( $\eta B$ ), where a fraction  $\eta$  (bandwidth allocation coefficient) of the total bandwidth ( $B$ ) is allocated for direct transmission to user  $U_1$ , represented by signal  $s_1$ ; and Region-2 ( $(1 - \eta) B$ ), where the remaining bandwidth is shared between  $U_1$  and  $U_2$ , with signals  $s_1$  and  $s_2$  superimposed using NOMA, given by the equation  $\bar{s} = \sum_{i=1}^2 \sqrt{\alpha_i} s_i$ . The power allocation factors  $\alpha_1$  and  $\alpha_2$  determine how power is distributed between the users, ensuring efficient resource utilization, satisfying the conditions  $\alpha_1 + \alpha_2 = 1$  and  $\alpha_2 > \alpha_1$ . This partial NOMA approach enhances spectral efficiency and user fairness by dynamically adjusting bandwidth and power allocation, making it a promising technique for BD-assisted NOMA-based wireless networks.

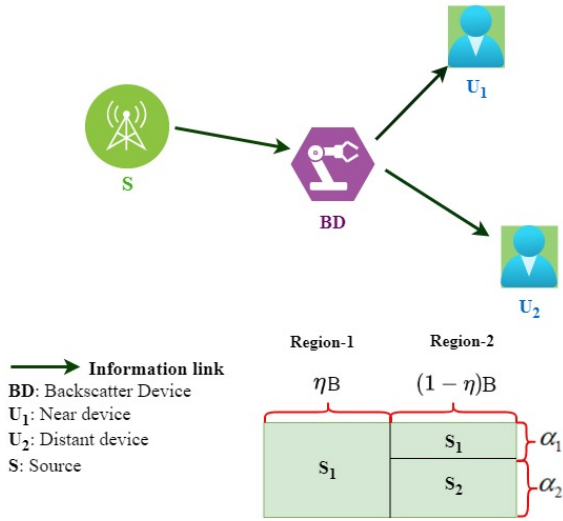


Fig. 1: System model

The BD reflects the S's signal to both users ( $U_1, U_2$ ) with its own message  $c(t)$  satisfying  $E\{|c(t)|^2\} = 1$ . The received signal at both users in region-1 and region-2 can be expressed as, respectively.

$$y_Q = \begin{cases} \sqrt{\eta} (\sqrt{\beta P_S} g_Q s_1(t) c(t) + n_Q), & \text{region - 1,} \\ \sqrt{1 - \eta} (\sqrt{\beta P_S} g_Q s_2(t) c(t) + n_Q), & \text{region - 2,} \end{cases} \quad (1)$$

where  $Q \in (U_1, U_2)$ ,  $\beta$  is reflection coefficient of BD,  $P_S$  is the transmit power of the S,  $n_Q$  is the independent additive white Gaussian noise (AWGN) with zero mean and variance of  $\sigma^2$ , and  $g_0, g_1, g_2$  are the channel coefficients of the links  $S \rightarrow BD$ ,  $BD \rightarrow U_1$ , and  $BD \rightarrow U_2$ , respectively, under a Rayleigh fading distribution.

Unlike conventional NOMA frameworks, it is assumed that  $U_1$  can aggregate all received signals to enhance decoding performance [53]. Based on (1) and the combination of both transmission regions, the instantaneous SINR at  $U_1$  for decoding its own message,  $s_1$ , is expressed as follows.

$$\begin{aligned} \gamma_{U_1} &= \frac{[\eta + (1 - \eta) \alpha_1] \beta P_S |g_0|^2 |g_1|^2}{(1 - \eta) \alpha_2 \beta P_S |g_0|^2 |g_1|^2 + \sigma^2} \\ &= \frac{[\eta + (1 - \eta) \alpha_1] \beta \psi |g_0|^2 |g_1|^2}{(1 - \eta) \alpha_2 \beta \psi |g_0|^2 |g_1|^2 + 1}, \end{aligned} \quad (2)$$

where  $\psi = \frac{P_S}{\sigma^2}$  is the average transmit signal-to-noise ratio (SNR). Further, conditioned on perfectly decoding  $s_1(t)$ ,  $U_1$  can then decode the backscatter signal  $c(t)$ , and the corresponding signal-to-noise ratio (SNR) to decode  $c(t)$  can be expressed as:

$$\gamma_{U_{1,c}} = (1 - \eta) \alpha_2 \beta \psi |g_0|^2 |g_1|^2. \quad (3)$$

Similarly, the SINR at  $U_2$  for decoding message  $s_2(t)$  from Region-2 is given by

$$\begin{aligned} \gamma_{U_2} &= \frac{(1 - \eta) \alpha_2 \beta P_S |g_0|^2 |g_2|^2}{(1 - \eta) \alpha_1 \beta P_S |g_0|^2 |g_2|^2 + (1 - \eta) \sigma^2} \\ &= \frac{\alpha_2 \beta \psi |g_0|^2 |g_2|^2}{\alpha_1 \beta \psi |g_0|^2 |g_2|^2 + 1}. \end{aligned} \quad (4)$$

$U_2$  can then decode the backscatter signal  $c(t)$ , and the corresponding SNR to decode  $c(t)$  can be expressed as:

$$\gamma_{U_{2,c}} = \alpha_1 \beta \psi |g_0|^2 |g_2|^2. \quad (5)$$

Finally, the BD signals can be successfully decoded when  $s_i(t)$  and  $c(t)$  are perfectly decoded at  $U_1$  and  $U_2$ . Thus, the end-to-end received SNR and SINR at  $U_1$  and  $U_2$  can be claimed by

$$\gamma_{U_1}^{e2e} = \min(\gamma_{U_1}, \gamma_{U_{1,c}}). \quad (6)$$

$$\gamma_{U_2}^{e2e} = \min(\gamma_{U_2}, \gamma_{U_{2,c}}). \quad (7)$$

### 3. Performance Analysis

In this section, the performances of the proposed system were analyzed. In particular, the closed-form of OP was derived.

#### 3.1. Channel model

In our analysis, we consider the channels between the source (S) and the backscatter device (BD), and between the BD and the users ( $U_1, U_2$ ), to be subject to Rayleigh fading. Specifically, the channel coefficients  $g_0, g_1, g_2$ , representing the links  $S \rightarrow BD$ ,  $BD \rightarrow U_1$ , and  $BD \rightarrow U_2$ , respectively, are modeled as independent Rayleigh fading random variables. The distinction in distributions arises from the differing path-loss effects, which are distance-dependent.

The probability density function (PDF) and the cumulative distribution function (CDF) of  $|g_i|^2$ ,  $\left(i = \begin{cases} 0, \text{ SB} \\ 1, \text{ BU}_1 \\ 2, \text{ BU}_2 \end{cases}\right)$  can be expressed as

$$\begin{aligned} f_{|g_i|^2}(x) &= \lambda_i \exp(-\lambda_i x) \\ F_{|g_i|^2}(x) &= 1 - \exp(-\lambda_i x), \end{aligned} \quad (8)$$

where  $\lambda_i$  is the mean of  $|g_i|^2$ .

To take into account the simple path-loss model,  $\lambda_i$  can be modeled by  $\lambda_i = (d_i)^\delta$ , where  $d_i$  is the distance between two correspondence nodes, and  $\delta$  is the path-loss exponent.

The PDF and CDF of the product of two squared Rayleigh random variables,  $\theta_i = |g_0|^2 |g_i|^2$  can be obtained as [54]

$$F_{\theta_i}(x) = 1 - 2\sqrt{\lambda_{SB}\lambda_i x} \times K_1\left(2\sqrt{\lambda_{SB}\lambda_i x}\right), \quad (9)$$

where  $K_1(\cdot)$  is the modified Bessel function of the second kind with 1<sup>th</sup> order. By using the formula  $\frac{d}{dx}(x^v K_v(x)) = -x^v K_{v-1}(x)$ , we have:

$$f_{\theta_i}(x) = 2\lambda_{SB}\lambda_i \times K_0\left(2\sqrt{\lambda_{SB}\lambda_i x}\right). \quad (10)$$

### 3.2. Outage Analysis at $U_1$

The OP of  $U_1$  can be thus defined by:

$$\begin{aligned} OP_1 &= \Pr(\gamma_{U_1}^{e2e} \leq \gamma_{th}) = \Pr(\min(\gamma_{U_1}, \gamma_{U_{1,c}}) \leq \gamma_{th}) \\ &= 1 - \Pr(\gamma_{U_1} \geq \gamma_{th}, \gamma_{U_{1,c}} \geq \gamma_{th}), \end{aligned} \quad (11)$$

where  $\gamma_{th}$  is threshold of the system. From (2) and (3), the OP at  $U_1$  can be reformulated as

$$\begin{aligned} OP_1 &= 1 - \Pr\left(\begin{aligned} &\frac{[\eta + (1 - \eta)\alpha_1]\beta\psi\theta_1}{(1 - \eta)\alpha_2\beta\psi\theta_1 + 1} \geq \gamma_{th}, \\ &(1 - \eta)\alpha_2\beta\psi\theta_1 \geq \gamma_{th} \end{aligned}\right) \\ &= 1 - \Pr\left(\begin{aligned} &\theta_1 \geq \underbrace{\frac{\gamma_{th}}{\beta\psi[\eta + (1 - \eta)(\alpha_1 - \alpha_2)]}}_{\Xi_1}, \\ &\theta_1 \geq \underbrace{\frac{\gamma_{th}}{(1 - \eta)\alpha_2\beta\psi}}_{\Xi_2} \end{aligned}\right). \end{aligned} \quad (12)$$

To ensure a comprehensive analysis, it is essential to consider both possible cases where one side of the inequality is greater or smaller than the other. Since the expressions are constrained by multiple parameters, examining both scenarios allows for a thorough evaluation of the constraint conditions that  $\theta_1$  must satisfy.

#### 1) Case 1: $\Xi_1 \geq \Xi_2$

If  $\Xi_1 \geq \Xi_2$ , the  $OP_1$  can be expressed as

$$\begin{aligned} OP_1 &= 1 - \Pr\left(\theta_1 \geq \underbrace{\frac{\gamma_{th}}{\beta\psi[\eta + (1 - \eta)(\alpha_1 - \alpha_2\gamma_{th})]}}_{\Xi_1}\right) \\ &= 1 - \Pr\left[1 - F_{\theta_1}\left(\frac{\gamma_{th}}{\beta\psi[\eta + (1 - \eta)(\alpha_1 - \alpha_2\gamma_{th})]}\right)\right]. \end{aligned} \quad (13)$$

By substituting (9) into (13), we obtain:

$$OP_1 = 1 - \left[2\sqrt{\frac{\gamma_{th}\lambda_{SB}\lambda_{BU_1}}{\beta\psi[\eta + (1 - \eta)(\alpha_1 - \alpha_2\gamma_{th})]}} \times K_1\left(2\sqrt{\frac{\gamma_{th}\lambda_{SB}\lambda_{BU_1}}{\beta\psi[\eta + (1 - \eta)(\alpha_1 - \alpha_2\gamma_{th})]}}\right)\right]. \quad (14)$$

#### 2) Case 2: $\Xi_1 < \Xi_2$

If  $\Xi_2 \geq \Xi_1$ , the  $OP_1$  can be expressed as

$$\begin{aligned} OP_1 &= 1 - \Pr\left(\theta_1 \geq \underbrace{\frac{\gamma_{th}}{(1 - \eta)\alpha_2\beta\psi}}_{\Xi_2}\right) \\ &= 1 - \Pr\left[1 - F_{\theta_1}\left(\frac{\gamma_{th}}{(1 - \eta)\alpha_2\beta\psi}\right)\right]. \end{aligned} \quad (15)$$

By substituting (9) into (15), we obtain:

$$OP_1 = 1 - \left[2\sqrt{\frac{\gamma_{th}\lambda_{SB}\lambda_{BU_1}}{(1 - \eta)\alpha_2\beta\psi}} \times K_1\left(2\sqrt{\frac{\gamma_{th}\lambda_{SB}\lambda_{BU_1}}{(1 - \eta)\alpha_2\beta\psi}}\right)\right]. \quad (16)$$

### 3.3. Outage Analysis at $U_2$

The OP of  $U_2$  can be thus defined by:

$$\begin{aligned} OP_2 &= \Pr(\gamma_{U_2}^{e2e} \leq \gamma_{th}) \\ &= \Pr(\min(\gamma_{U_2}, \gamma_{U_{2,c}}) \leq \gamma_{th}) \\ &= 1 - \Pr(\gamma_{U_2} \geq \gamma_{th}, \gamma_{U_{2,c}} \geq \gamma_{th}). \end{aligned} \quad (17)$$

From (4) and (5), the OP at  $U_2$  can be reformulated as

$$\begin{aligned} OP_2 &= 1 - \Pr\left(\begin{aligned} &\frac{\alpha_2\beta\psi\theta_2}{\alpha_1\beta\psi\theta_2 + 1} \geq \gamma_{th}, \\ &\alpha_1\beta\psi\theta_2 \geq \gamma_{th} \end{aligned}\right) \\ &= 1 - \Pr\left(\begin{aligned} &\theta_2 \geq \underbrace{\frac{\gamma_{th}}{\beta\psi(\alpha_2 - \alpha_1\gamma_{th})}}_{\Omega_1}, \\ &\theta_2 \geq \underbrace{\frac{\gamma_{th}}{\alpha_1\beta\psi}}_{\Omega_2} \end{aligned}\right). \end{aligned} \quad (18)$$

1) **Case 1:**  $\Omega_1 \geq \Omega_2$

If  $\Omega_1 \geq \Omega_2$ , the  $OP_2$  can be expressed as

$$OP_2 = 1 - \Pr \left( \theta_2 \geq \underbrace{\frac{\gamma_{th}}{\beta\psi(\alpha_2 - \alpha_1\gamma_{th})}}_{\Omega_1} \right) \tag{19}$$

$$= 1 - \left[ 1 - F_{\theta_2} \left( \frac{\gamma_{th}}{\beta\psi(\alpha_2 - \alpha_1\gamma_{th})} \right) \right].$$

By substituting (9) into (19), we obtain:

$$OP_2 = 1 - \left[ 2\sqrt{\frac{\gamma_{th}\lambda_{SB}\lambda_{BU_2}}{\beta\psi(\alpha_2 - \alpha_1\gamma_{th})}} \times K_1 \left( 2\sqrt{\frac{\gamma_{th}\lambda_{SB}\lambda_{BU_2}}{\beta\psi(\alpha_2 - \alpha_1\gamma_{th})}} \right) \right]. \tag{20}$$

2) **Case 2:**  $\Omega_2 \geq \Omega_1$

If  $\Omega_2 \geq \Omega_1$ , the  $OP_2$  can be expressed as

$$OP_2 = 1 - \Pr \left( \theta_2 \geq \underbrace{\frac{\gamma_{th}}{\alpha_1\beta\psi}}_{\Omega_2} \right) \tag{21}$$

$$= 1 - \left[ 1 - F_{\theta_2} \left( \frac{\gamma_{th}}{\alpha_1\beta\psi} \right) \right].$$

By substituting (9) into (21), we obtain:

$$OP_2 = 1 - \left[ 2\sqrt{\frac{\gamma_{th}\lambda_{SB}\lambda_{BU_2}}{\alpha_1\beta\psi}} \times K_1 \left( 2\sqrt{\frac{\gamma_{th}\lambda_{SB}\lambda_{BU_2}}{\alpha_1\beta\psi}} \right) \right]. \tag{22}$$

### 3.4. Overall Outage Analysis

The OP of the entire system is given by the product of the OP at user  $U_1$  and the OP at user  $U_2$ , expressed as [61]:

$$OP = 1 - (1 - OP_1) \times (1 - OP_2). \tag{23}$$

The OP of the system also varies according to the constraint conditions, as observed in section 3.2. and 3.3. . Therefore, the OP is specifically expressed as follows:

$$\left\{ \begin{array}{l} \Xi_1 \geq \Xi_2 \\ \Xi_1 \leq \Xi_2 \end{array} \right\} \left\{ \begin{array}{l} \Omega_1 \geq \Omega_2 \rightarrow OP = OP_{case\_1} \\ \Omega_1 \leq \Omega_2 \rightarrow OP = OP_{case\_2} \\ \Omega_1 \geq \Omega_2 \rightarrow OP = OP_{case\_3} \\ \Omega_1 \leq \Omega_2 \rightarrow OP = OP_{case\_4} \end{array} \right. , \tag{24}$$

with OP for all cases expressed sequentially as follows:

$$OP_{case\_1} = 1 - \frac{4\gamma_{th}\lambda_{SB}}{\beta\psi} \times \sqrt{\frac{\lambda_{BU_1}\lambda_{BU_2}}{[\eta + (1 - \eta)(\alpha_1 - \alpha_2\gamma_{th})](\alpha_2 - \alpha_1\gamma_{th})}} \times K_1 \left( 2\sqrt{\frac{\gamma_{th}\lambda_{SB}\lambda_{BU_1}}{\beta\psi[\eta + (1 - \eta)(\alpha_1 - \alpha_2\gamma_{th})]}} \right) \times K_1 \left( 2\sqrt{\frac{\gamma_{th}\lambda_{SB}\lambda_{BU_2}}{\beta\psi(\alpha_2 - \alpha_1\gamma_{th})}} \right). \tag{25}$$

$$OP_{case\_2} = 1 - \frac{4\gamma_{th}\lambda_{SB}}{\beta\psi} \times \sqrt{\frac{\lambda_{BU_1}\lambda_{BU_2}}{\alpha_1[\eta + (1 - \eta)(\alpha_1 - \alpha_2\gamma_{th})]}} \times K_1 \left( 2\sqrt{\frac{\lambda_{BU_1}}{\beta\psi[\eta + (1 - \eta)(\alpha_1 - \alpha_2\gamma_{th})]}} \right) \times K_1 \left( 2\sqrt{\frac{\gamma_{th}\lambda_{SB}\lambda_{BU_2}}{\alpha_1\beta\psi}} \right). \tag{26}$$

$$OP_{case\_3} = 1 - \frac{4\gamma_{th}\lambda_{SB}}{\beta\psi} \sqrt{\frac{\lambda_{BU_1}\lambda_{BU_2}}{(\alpha_2 - \alpha_1\gamma_{th})(1 - \eta)\alpha_2}} \times K_1 \left( 2\sqrt{\frac{\gamma_{th}\lambda_{SB}\lambda_{BU_1}}{(1 - \eta)\alpha_2\beta\psi}} \right) K_1 \left( 2\sqrt{\frac{\gamma_{th}\lambda_{SB}\lambda_{BU_2}}{\beta\psi(\alpha_2 - \alpha_1\gamma_{th})}} \right). \tag{27}$$

$$OP_{case\_4} = 1 - \frac{4\gamma_{th}\lambda_{SB}}{\beta\psi} \sqrt{\frac{\lambda_{BU_1}\lambda_{BU_2}}{(1 - \eta)\alpha_1\alpha_2}} \times K_1 \left( 2\sqrt{\frac{\gamma_{th}\lambda_{SB}\lambda_{BU_1}}{(1 - \eta)\alpha_2\beta\psi}} \right) \times K_1 \left( 2\sqrt{\frac{\gamma_{th}\lambda_{SB}\lambda_{BU_2}}{\alpha_1\beta\psi}} \right). \tag{28}$$

## 4. Numerical results

This section presents numerical results to validate the accuracy of the proposed mathematical models and analyze the system's behavior under different key parameters using the Monte Carlo approach [55–58]. The simulation parameters are detailed in Table 1.

The figure 2 illustrates the relationship between the OP and the average signal power  $\psi$ (dB), while also

**Tab. 1:** Simulation parameters.

Symbol	Parameter name	Value
$\gamma_{th}$	Threshold of the system	0.1:1.25
$\alpha_1$	Power allocation ratio at $U_1$	0.05:0.5
$\alpha_2$	Power allocation ratio at $U_2$	$1 - \alpha_1$
$\eta$	Bandwidth allocation coefficient	0; 0.5; 0.75
$\beta$	The backscatter efficiency	0.5
$d_{SB}$	Distance between S and BD	1; 2; 3m
$d_{BU_1}$	Distance between BD and $U_1$	2m
$d_{BU_2}$	Distance between BD and $U_2$	1m
$\delta$	Path-loss exponent	2
$\psi$	Average transmit power to noise ratio at source	-10 to 50 (dB)

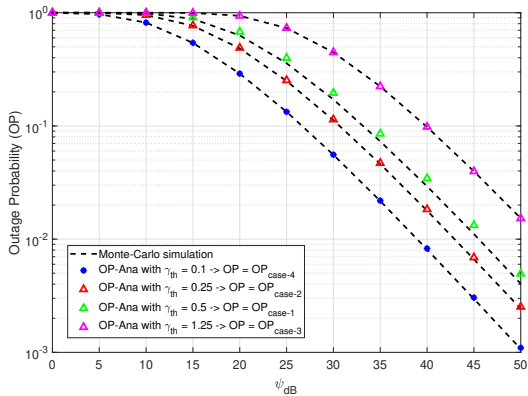


**Fig. 2:** The OP versus  $\psi$ (dB) with varying the threshold of the system  $\gamma_{th}$ .

considering the impact of the system threshold  $\gamma_{th}$ . The plot includes a dashed line representing Monte Carlo simulation results that confirm the accuracy of the analytical expressions and markers corresponding to different values of  $\gamma_{th}$ . The results indicate that as  $\psi_{dB}$  increases, OP significantly decreases. This is because higher signal power improves the received signal quality, enhances the decoding capability, and reduces the likelihood of communication failure. However, when  $\gamma_{th}$  increases from 0.1 to 1.25, OP also increases. A higher system threshold imposes stricter signal quality requirements for successful decoding, making it more difficult for the system to maintain a stable connection. As a result, the probability of outage increases. Different  $\gamma_{th}$  values correspond to different OP curves, labeled as  $OP_{case\_1}$ ,  $OP_{case\_2}$ ,  $OP_{case\_3}$ , and  $OP_{case\_4}$ . Among these,  $OP_{case\_4}$  (corresponding to  $\gamma_{th} = 0.1$ ) achieves the lowest OP, meaning it provides better system performance. In contrast,  $OP_{case\_3}$  (corresponding to  $\gamma_{th} = 1.25$ ) exhibits the highest OP, indicating degraded performance. These findings highlight the trade-off between system threshold selection and communication reliability. While increasing  $\psi$ (dB) generally improves system perfor-

mance, choosing an appropriate  $\gamma_{th}$  is crucial to avoid excessive OP.

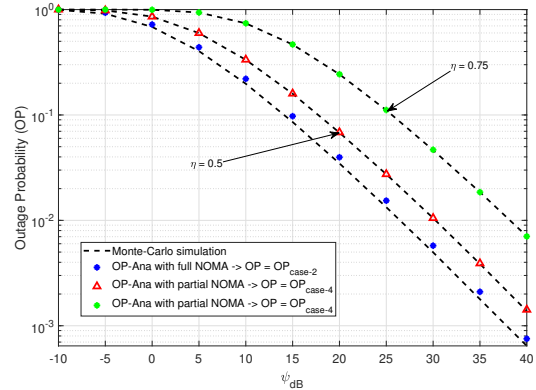


**Fig. 3:** The OP versus  $\psi$ (dB) with varying the threshold of the system  $\gamma_{th}$  and bandwidth allocation coefficient  $\eta$ .

The figure 3 illustrates the relationship between the OP and the average signal power  $\psi$ (dB), while also considering the impact of the bandwidth allocation coefficient  $\eta$ . Monte Carlo simulations are employed to verify the accuracy of the analytical expressions. The results indicate that as  $\psi$ (dB) increases, OP decreases significantly due to higher signal power, which enhances channel quality, improves signal decoding capability, and reduces the risk of outage, similar to the observations in Fig.2. Additionally, the bandwidth allocation coefficient  $\eta$  significantly impacts system performance. When  $\eta$  increases from 0 to 0.75, OP tends to increase, indicating that proper bandwidth allocation enhances signal quality and optimizes transmission efficiency. When  $\eta = 0$ , the entire bandwidth is allocated for non-orthogonal access, and the system operates under a full NOMA scheme. In this case, both users are served simultaneously over the same spectrum, and the near user applies successive interference cancellation (SIC) to decode its message. By utilizing the entire spectrum, full NOMA allows boosting overall system throughput and performance. However, as  $\eta$  increases, the system transitions to a partial NOMA configuration, and now the OP increases significantly. This result can be explained by the fact that although partial NOMA does not utilize the entire spectrum simultaneously like full NOMA, it achieves more efficient spectrum usage by enabling flexible resource allocation, mitigating inter-user interference, and reducing power consumption and processing complexity. This makes partial NOMA especially suitable for energy-constrained devices such as backscatter devices. Nonetheless, this does not diminish the value of full NOMA, particularly in scenarios where maximizing spectrum utilization is a priority. Since spectrum is a highly limited and valuable resource in wireless communication systems, the choice between full NOMA and partial NOMA should be made carefully, based

on the trade-offs between spectrum efficiency, receiver complexity, and application-specific requirements.

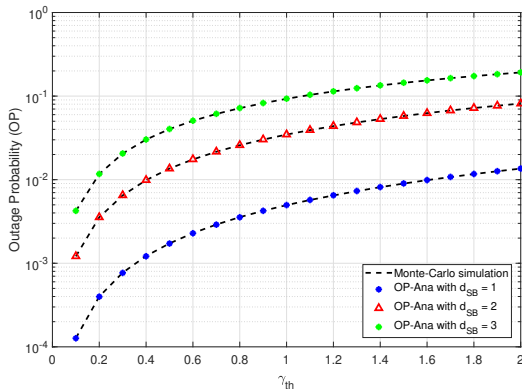


**Fig. 4:** The OP versus the system  $\gamma_{th}$  with varying the distance  $S$  to BD  $d_{SB}$ .

The figure 4 presents the impact of the system threshold  $\gamma_{th}$  and the distance from the source  $SS$  to the backscatter device  $BD(d_{SB})$  on the OP. The dashed lines represent the Monte Carlo simulation results, while the markers correspond to the analytical results. The results indicate that as  $\gamma_{th}$  increases, OP also rises significantly. This is because a higher system threshold requires a stronger received signal to maintain communication, leading to a higher risk of outage if the signal quality is insufficient, as previously discussed in Figures 2 and 3. Moreover, the distance  $d_{SB}$  plays a crucial role in OP performance. As  $d_{SB}$  increases from 1 to 3m, OP also rises considerably. This is due to the fact that a greater distance between the source and BD results in higher path loss, which weakens the backscattered signal. Consequently, the received signal quality at both BD and the destination degrades, reducing the ability to decode the information and thereby increasing OP. In summary, these findings emphasize the importance of selecting an appropriate system threshold  $\gamma_{th}$  to prevent excessive OP growth. Additionally, optimizing the source-to-BD distance is essential for maintaining an efficient system performance.

Figure 5 illustrates the relationship between the OP and the power allocation coefficient  $\alpha_1$  at user  $U_1$ , considering different values of  $\psi_{dB}$ . Similar to Figure 2, OP decreases as  $\psi_{dB}$  increases, indicating that stronger signal power enhances system reliability and reduces the risk of communication failure. Regarding the impact of power allocation  $\alpha_1$ , OP exhibits a non-monotonic trend. Specifically, as  $\alpha_1$  increases from 0.05 to approximately 0.25 - 0.35, OP decreases, suggesting that allocating more power to user  $U_1$  within this range improves system performance. However, when  $\alpha_1$  further increases toward 0.5, OP starts rising again. This suggests that an optimal value of  $\alpha_1$  exists to minimize OP. The reason behind this behavior lies in the balance

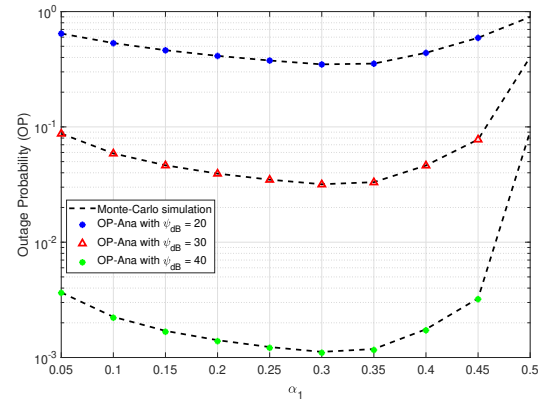


**Fig. 5:** The OP versus power allocation ratios  $\alpha_1$  with varying  $\psi$ (dB).

between power allocation for user  $U_1$  and the remaining users in the system. If  $\alpha_1$  is too small,  $U_1$  receives insufficient power, degrading signal quality and increasing OP. Conversely, if  $\alpha_1$  is too large, the remaining users receive less power, negatively impacting overall system performance and raising OP. In summary, OP decreases as  $\psi$ (dB) increases, consistent with Figure 2. Additionally, OP depends on  $\alpha_1$ , where an optimal allocation minimizes OP. Thus, selecting an appropriate  $\alpha_1$  value is crucial to optimizing system performance and reducing outage risk.

## 5. Conclusion

In this study, we analyzed the OP of a backscatter-assisted partial NOMA system, where a BD reflects signals to multiple users. We derived closed-form expressions for the OP under different decoding conditions and evaluated the impact of system parameters on performance. The results demonstrate that integrating BackCom with partial NOMA enhances system reliability and spectral efficiency compared to conventional approaches. Notably, the power allocation factor  $\alpha_1$  plays a crucial role in balancing performance between users. We observed that OP does not decrease uniformly with  $\alpha_1$  but has an optimal value that minimizes OP most effectively. This highlights the importance of selecting an appropriate  $\alpha_1$  to ensure signal quality for both users, avoiding scenarios where one user experiences significant performance degradation due to improper power allocation. For future research, several directions can be explored. First, extending the current model to account for imperfect channel state information (CSI) could provide more practical insights. Additionally, investigating the impact of multiple BD devices and cooperative backscattering relaying strategies may further enhance system performance. Finally, optimizing power allocation and resource management

through machine learning-based approaches could pave the way for intelligent and adaptive BackCom-NOMA systems in next-generation wireless networks.

## Acknowledgment

This research is supported by Posts and Telecommunications Institute of Technology (PTIT).

## Author Contributions

Both Thu-Ha Thi Pham and Quoc Su Nguyen carried out analytical computations and numerical simulations. Nhat Truong Thanh Nguyen and Thu-Ha Thi Pham wrote the whole paper. While Thanh Hon Nguyen, Bui Vu Minh, and Quang-Sang Nguyen developed the system model and proposed the idea. Finally, Minh Tran supervises this work. All authors contributed to the final version of the manuscript.

## References

- [1] ZHANG, L., M. XIAO, G. WU, M. ALAM, Y.-C. LIANG and S. LI. A Survey of Advanced Techniques for Spectrum Sharing in 5G Networks. *IEEE Wireless Communications*. 2017, vol. 24, iss. 5, pp. 44–51. ISSN 1536-1284. DOI: 10.1109/MWC.2017.1700069.
- [2] DING, Z., X. LEI, G. K. KARAGIANNIDIS, R. SCHOBBER, J. YUAN and V. BHARGAVA. A Survey on Non-Orthogonal Multiple Access for 5G Networks: Research Challenges and Future Trends. *IEEE Journal on Selected Areas in Communications*. 2017, vol. 35, iss. 10, pp. 2181–2195. ISSN 0733-8716. DOI: 10.1109/JSAC.2017.2725519.
- [3] NGUYEN, N.-T., H.-N. NGUYEN, N.-L. NGUYEN, A.-T. LE, T. N. NGUYEN and M. VOZNAK. Performance Analysis of NOMA-Based Hybrid Satellite-Terrestrial Relay System Using mmWave Technology. *IEEE Access*. 2023, vol. 11, pp. 10696–10707. DOI: 10.1109/ACCESS.2023.3238335.
- [4] TU, L.-T., V.-D. PHAN, T. N. NGUYEN, P. T. TRAN, T. T. DUY, Q.-S. NGUYEN, N.-T. NGUYEN and M. VOZNAK. Performance Analysis of Multihop Full-Duplex NOMA Systems with Imperfect Interference Cancellation and Near-Field Path-Loss. *Sensors*. 2023, vol. 23, no. 1, article no. 524. ISSN 1424-8220. DOI: 10.3390/s23010524.
- [5] YOU, X., C. ZHANG, X. TAN, S. JIN and H. WU. AI for 5G: Research Directions and Paradigms. *Science China Information Sciences*. 2019, vol. 62, iss. 2, pp. 21301. ISSN 1674-733X. DOI: 10.1007/s11432-018-9596-5.
- [6] ZHOU, F., Y. WU, Y.-C. LIANG, Z. LI, Y. WANG and K.-K. WONG. State of the Art Taxonomy and Open Issues on Cognitive Radio Networks With NOMA. *IEEE Wireless Communications*. 2018, vol. 25, iss. 2, pp. 100–108. ISSN 1536-1284. DOI: 10.1109/MWC.2018.1700113.
- [7] LUONG, N. C., P. WANG, D. NIYATO, Y.-C. LIANG, Z. HAN and F. HOU. Applications of Economic and Pricing Models for Resource Management in 5G Wireless Networks: A Survey. *IEEE Communications Surveys & Tutorials*. DOI: 10.1109/COMST.2018.2870996.
- [8] LIU, X., H. DING and S. HU. Uplink Resource Allocation for NOMA-Based Hybrid Spectrum Access in 6G-Enabled Cognitive Internet of Things. *IEEE Internet of Things Journal*. 2021, vol. 8, iss. 20, pp. 15049–15058. ISSN 2327-4662. DOI: 10.1109/JIOT.2020.3007017.
- [9] ZHANG, N., J. WANG, G. KANG and Y. LIU. Uplink Non-Orthogonal Multiple Access in 5G Systems. *IEEE Communications Letters*. 2016, vol. 20, iss. 3, pp. 458–461. ISSN 1089-7798. DOI: 10.1109/LCOMM.2016.2521374.
- [10] SUN, Q., S. HAN, C. L. I and Z. PAN. On the ergodic capacity of MIMO NOMA systems. *IEEE Wireless Communications Letters*. 2015, vol. 4, iss. 4, pp. 405–408. ISSN 2162-2337. DOI: 10.1109/LWC.2015.2426709.
- [11] DING, Z., F. ADACHI and H. V. POOR. The application of MIMO to non-orthogonal multiple access. *IEEE Transactions on Wireless Communications*. 2016, vol. 15, iss. 1, pp. 537–552. ISSN 1536-1276. DOI: 10.1109/TWC.2015.2475746.
- [12] PHU, L. S., T. N. NGUYEN, M. VOZNAK, B. C. NGUYEN, T. M. HOANG, B. V. MINH and P. T. TRAN. Improving the Capacity of NOMA Network Using Multiple Aerial Intelligent Reflecting Surfaces. *IEEE Access*. 2023, vol. 11, pp. 107958–107971. DOI: 10.1109/ACCESS.2023.3319675.
- [13] ZENG, M., A. YADAV, O. A. DOBRE, G. I. TSIROPULOS and H. V. POOR. Capacity Comparison Between MIMO-NOMA and MIMO-NOMA With Multiple Users in a Cluster. *IEEE Journal on Selected Areas in Communications*. 2017, vol. 35, iss. 10, pp. 2413–2424. ISSN 0733-8716. DOI: 10.1109/JSAC.2017.2725879.

- [14] HUNG, T. C., B. V. MINH, T. N. NGUYEN and M. VOZNAK. Power beacon-assisted energy harvesting symbiotic radio networks: Outage performance. *PLOS ONE*. 2025, vol. 20, iss. 2, pp. 1–16. DOI: 10.1371/journal.pone.0313981.
- [15] LE, A. T., T. H. VU, N. H. TU, T. N. NGUYEN, L. T. TU and M. VOZNAK. Active Reconfigurable Repeater-Assisted NOMA Networks in Internet-of-Things: Reliability, Security, and Covertness. *IEEE Internet of Things Journal*. 2024, pp. 1–1. DOI: 10.1109/JIOT.2024.3503278.
- [16] VU, T. H., T. N. NGUYEN, T. T. NGUYEN and S. KIM. Hybrid Active-Passive STAR-RIS-Based NOMA Systems: Energy/Rate-Reliability Trade-Offs and Rate Adaptation. *IEEE Wireless Communications Letters*. 2025, vol. 14, iss. 1, pp. 238–242. DOI: 10.1109/LWC.2024.3497978.
- [17] HUNG, T. C., T. N. NGUYEN, N. H. K. NHAN, A. T. LE, P. N. SON, T. H. T. PHAM and M. VOZNAK. Performance analysis of dual-hop mixed RF-FSO systems combined with NOMA. *PLOS ONE*. 2024, vol. 19, iss. 12, pp. 1–19. DOI: 10.1371/journal.pone.0315123.
- [18] HUNG, T. C., T. N. NGUYEN, Q. S. VU, A. T. LE, B. V. MINH and M. VOZNAK. Performance Analysis of Ergodic Rate and Effective Capacity for RIS-Assisted NOMA Networks Over Nakagami-m Fading Environments. *IEEE Access*. 2024, vol. 12, pp. 181271–181281. DOI: 10.1109/ACCESS.2024.3509856.
- [19] LIU, Y., Z. QIN, M. ELKASHLAN, A. NALANATHAN and J. A. McCANN. Non-Orthogonal Multiple Access in Large-Scale Heterogeneous Networks. *IEEE Journal on Selected Areas in Communications*. 2017, vol. 35, iss. 12, pp. 2667–2680. ISSN 0733-8716. DOI: 10.1109/JSAC.2017.2726718.
- [20] ZENG, M., G. I. TSIROPULOS, O. A. DOBRE and M. H. AHMED. Power Allocation for Cognitive Radio Networks Employing Non-Orthogonal Multiple Access. In: *2016 IEEE Global Communications Conference (GLOBECOM)*, Washington, DC, USA, 2016, pp. 1–5. DOI: 10.1109/GLOCOM.2016.7842156.
- [21] PHAM, X. N., B. C. NGUYEN, T. D. THI, N. V. VINH, B. V. MINH, T. KIM, T. N. NGUYEN and A. V. LE. Enhancing data rate and energy efficiency of NOMA systems using reconfigurable intelligent surfaces for millimeter-wave communications. *Digital Signal Processing*. 2024, vol. 151, pp. 104553. DOI: 10.1016/j.dsp.2024.104553.
- [22] VO, D. T., T. N. NGUYEN, A. T. LE, V. D. PHAN and M. VOZNAK. Holographic Reconfigurable Intelligent Surface-Aided Downlink NOMA IoT Networks in Short-Packet Communication. *IEEE Access*. 2024, vol. 12, pp. 65266–65277. DOI: 10.1109/ACCESS.2024.3397306.
- [23] LE, A. T., T. D. HIEU, T. N. NGUYEN, T. L. LE, S. Q. NGUYEN and M. VOZNAK. Physical layer security analysis for RIS-aided NOMA systems with non-colluding eavesdroppers. *Computer Communications*. 2024, vol. 219, pp. 194–203. DOI: 10.1016/j.comcom.2024.03.011.
- [24] LE, A. T., T. N. NGUYEN, L. T. TU, T. T. PHU, T. T. DUY, M. VOZNAK and Z. DING. Performance Analysis of RIS-Assisted Ambient Backscatter Communication Systems. *IEEE Wireless Communications Letters*. 2024, vol. 13, iss. 3, pp. 791–795. DOI: 10.1109/LWC.2023.3344113.
- [25] LE, A. T., T. D. HIEU, C. B. LE, T. T. PHU, T. N. NGUYEN, Z. DING, H. V. POOR and M. VOZNAK. Power Beacon and NOMA-Assisted Cooperative IoT Networks with Co-Channel Interference: Performance Analysis and Deep Learning Evaluation. *IEEE Transactions on Mobile Computing*. 2024, vol. 23, iss. 6, pp. 7270–7283. DOI: 10.1109/TMC.2023.3333764.
- [26] NGUYEN, Q.-S., T. N. NGUYEN and L.-T. TU. On the security and reliability performance of SWIPT-enabled full-duplex relaying in the non-orthogonal multiple access networks. *Journal of Information and Telecommunication*. 2023, vol. 7, no. 4, pp. 462–476. Taylor & Francis. DOI: 10.1080/24751839.2023.2218046.
- [27] NGUYEN, H., T. N. NGUYEN, B. V. MINH, T. H. T. PHAM, A. T. LE and M. VOZNAK. Security-Reliability Analysis in CR-NOMA IoT Network Under I/Q Imbalance. *IEEE Access*. 2023, vol. 11, pp. 119045–119056. DOI: 10.1109/ACCESS.2023.3327789.
- [28] LI, X., J. LI, Y. LIU, Z. DING and A. NALANATHAN. Residual Transceiver Hardware Impairments on Cooperative NOMA Networks. *IEEE Transactions on Wireless Communications*. 2020, vol. 19, iss. 1, pp. 680–695. ISSN 1536-1276. DOI: 10.1109/TWC.2019.2947670.
- [29] NGUYEN, N.-P., M. ZENG, O. A. DOBRE and H. V. POOR. Securing Massive MIMO-NOMA Networks with ZF Beamforming and Artificial Noise. In: *2019 IEEE Global Communications Conference (GLOBECOM)*, Waikoloa, HI, USA, 2019, pp. 1–6. DOI: 10.1109/GLOBECOM38437.2019.9013326.

- [30] ZENG, M., N.-P. NGUYEN, O. A. DOBRE and H. V. POOR. Securing Downlink Massive MIMO-NOMA Networks With Artificial Noise. *IEEE Journal of Selected Topics in Signal Processing*. 2019, vol. 13, iss. 3, pp. 685–699. ISSN 1932-4553. DOI: 10.1109/JSTSP.2019.2901170.
- [31] LEI, H. et al. Secrecy Outage Analysis for Cooperative NOMA Systems With Relay Selection Schemes. *IEEE Transactions on Communications*. 2019, vol. 67, iss. 9, pp. 6282–6298. ISSN 0090-6778. DOI: 10.1109/TCOMM.2019.2916070.
- [32] LI, B., X. QI, K. HUANG, Z. FEI, F. ZHOU and R. Q. HU. Security-Reliability Tradeoff Analysis for Cooperative NOMA in Cognitive Radio Networks. *IEEE Transactions on Communications*. 2019, vol. 67, iss. 1, pp. 83–96. ISSN 0090-6778. DOI: 10.1109/TCOMM.2018.2873690.
- [33] DING, Z., R. SCHOBBER and H. V. POOR. A general MIMO framework for NOMA downlink and uplink transmission based on signal alignment. *IEEE Transactions on Wireless Communications*. 2016, vol. 15, iss. 6, pp. 4438–4454. ISSN 1536-1276. DOI: 10.1109/TWC.2016.2542066.
- [34] JACOB, S. et al. A Novel Spectrum Sharing Scheme Using Dynamic Long Short-Term Memory With CP-OFDMA in 5G Networks. *IEEE Transactions on Cognitive Communications and Networking*. 2020, vol. 6, iss. 3, pp. 926–934. ISSN 2332-7731. DOI: 10.1109/TCCN.2020.2970697.
- [35] CHOI, J. Power Allocation for Max-Sum Rate and Max-Min Rate Proportional Fairness in NOMA. *IEEE Communications Letters*. 2016, vol. 20, iss. 10, pp. 2055–2058. ISSN 1089-7798. DOI: 10.1109/LCOMM.2016.2596760.
- [36] DING, Z., M. PENG and H. V. POOR. Cooperative non-orthogonal multiple access in 5G systems. *IEEE Communications Letters*. 2015, vol. 19, iss. 8, pp. 1462–1465. ISSN 1089-7798. DOI: 10.1109/LCOMM.2015.2441064.
- [37] LIU, Y., Z. DING, M. ELKASHLAN and H. V. POOR. Cooperative non-orthogonal multiple access with simultaneous wireless information and power transfer. *IEEE Journal on Selected Areas in Communications*. 2016, vol. 34, iss. 4, pp. 938–953. ISSN 0733-8716. DOI: 10.1109/JSAC.2016.2549378.
- [38] LU, X., D. NIYATO, H. JIANG, D. I. KIM, Y. XIAO, and Z. HAN. Ambient Backscatter Assisted Wireless Powered Communications. *IEEE Wireless Communications*. 2018, vol. 25, no. 2, pp. 170–177. DOI: 10.1109/MWC.2017.1600398.
- [39] LYU, B., Z. YANG, H. GUO, F. TIAN, and G. GUI. Relay Cooperation Enhanced Backscatter Communication for Internet-of-Things. *IEEE Internet of Things Journal*. 2019, vol. 6, no. 2, pp. 2860–2871. DOI: 10.1109/JIOT.2018.2875719.
- [40] LU, X., D. NIYATO, H. JIANG, E. HOS-SAIN, and P. WANG. Ambient Backscatter-Assisted Wireless-Powered Relaying. *IEEE Transactions on Green Communications and Networking*. 2019, vol. 3, no. 4, pp. 1087–1105. DOI: 10.1109/TGCN.2019.2936544.
- [41] DARSENA, D., G. GELLI, and F. VERDE. Modeling and Performance Analysis of Wireless Networks With Ambient Backscatter Devices. *IEEE Transactions on Communications*. 2017, vol. 65, no. 4, pp. 1797–1814. DOI: 10.1109/TCOMM.2017.2654448.
- [42] ZHAO, W., G. WANG, S. ATAPATTU, C. TELLAMBURA, and H. GUAN. Outage Analysis of Ambient Backscatter Communication Systems. *IEEE Communications Letters*. 2018, vol. 22, no. 8, pp. 1736–1739. DOI: 10.1109/LCOMM.2018.2842774.
- [43] GUO, J., X. ZHOU, S. DURRANI, and H. YANIKOMEROGLU. Design of Non-Orthogonal Multiple Access Enhanced Backscatter Communication. *IEEE Transactions on Wireless Communications*. 2018, vol. 17, no. 10, pp. 6837–6852. DOI: 10.1109/TWC.2018.2864741.
- [44] GUO, H., Y.-C. LIANG, R. LONG, and Q. ZHANG. Cooperative Ambient Backscatter System: A Symbiotic Radio Paradigm for Passive IoT. *IEEE Wireless Communications Letters*. 2019, vol. 8, no. 4, pp. 1191–1194. DOI: 10.1109/LWC.2019.2911500.
- [45] YE, Y., L. SHI, X. CHU, and G. LU. On the Outage Performance of Ambient Backscatter Communications. *IEEE Internet of Things Journal*. 2020, vol. 7, no. 8, pp. 7265–7278. DOI: 10.1109/JIOT.2020.2984449.
- [46] DASKALAKIS, S. N., A. GEORGIADIS, G. GOUSSETIS, and M. M. TENTZERIS. Low Cost Ambient Backscatter for Agricultural Applications. In: *2019 IEEE-APS Topical Conference on Antennas and Propagation in Wireless Communications (APWC)*. 2019, pp. 201–201. DOI: 10.1109/APWC.2019.8870568.
- [47] LU, X., H. JIANG, D. NIYATO, D. I. KIM, and Z. HAN. Wireless-Powered Device-to-Device Communications With Ambient Backscattering: Performance Modeling and Analysis. *IEEE Transactions on Wireless Com-*

- munications*. 2018, **17**(3), pp. 1528–1544. DOI: 10.1109/TWC.2017.2779857.
- [48] ZHANG, L., J. LIU, M. XIAO, G. WU, Y.-C. LIANG, and S. LI. Performance analysis and optimization in downlink NOMA systems with cooperative full-duplex relaying. *IEEE Journal on Selected Areas in Communications*. 2017, vol. 35, iss. 10, pp. 2398–2412. ISSN 0733-8716. DOI: 10.1109/JSAC.2017.2724678.
- [49] YANG, Q., H.-M. WANG, Q. YIN, and A. L. SWINDLEHURST. Exploiting Randomized Continuous Wave in Secure Backscatter Communications. *IEEE Internet of Things Journal*. 2020, **7**(4), pp. 3389–3403. DOI: 10.1109/JIOT.2020.2968337.
- [50] ZHANG, Y., F. GAO, L. FAN, X. LEI, and G. K. KARAGIANNIDIS. Secure Communications for Multi-Tag Backscatter Systems. *IEEE Wireless Communications Letters*. 2019, **8**(4), pp. 1146–1149. DOI: 10.1109/LWC.2019.2909199.
- [51] HAN, J. Y., M. J. KIM, J. KIM, and S. M. KIM. Physical Layer Security in Multi-Tag Ambient Backscatter Communications – Jamming vs. Cooperation. In: *Proc. IEEE Wireless Communications and Networking Conference (WCNC)*, 2020, pp. 1–6. DOI: 10.1109/WCNC45663.2020.9120481.
- [52] THUAN, D. H., N.-T. NGUYEN, X. T. NGUYEN, N. T. HAU, B. V. MINH, and T. N. NGUYEN. Uplink and downlink of energy harvesting NOMA system: performance analysis. *Journal of Information and Telecommunication*. 2024, vol. 8, no. 1, pp. 92–107. Taylor & Francis. DOI: 10.1080/24751839.2023.2260230.
- [53] AKHTAR, M. W., A. MAHMOOD, and M. GIDLUND. Partial NOMA for Semi-Integrated Sensing and Communication. In: *Proc. IEEE Globecom Workshops (GC Wkshps)*, 2023, pp. 1129–1134. DOI: 10.1109/GCWkshps58843.2023.10464754.
- [54] TRAN TIN, P., B. H. DINH, T. N. NGUYEN, D. H. HA, and T. T. TRANG. Power Beacon-Assisted Energy Harvesting Wireless Physical Layer Cooperative Relaying Networks: Performance Analysis. *Symmetry*, 2020, **12**(1), 106. DOI: 10.3390/sym12010106.
- [55] PHU T-T, TAN N. N, MINH TRAN, T.T TRANG, and L. SEVCIK. Exploiting Direct Link in Two-Way Half-Duplex Sensor Network over Block Rayleigh Fading Channel: Upper Bound Ergodic Capacity and Exact SER Analysis. *Sensors*. 2020, vol. 20, iss. 4, pp. 1–16. DOI: 10.3390/s20041165.
- [56] NGUYEN, T. N., T. TRAN, P., MINH, T. H. Q., VOZNAK, M., and SEVCIK, L. Two-Way Half Duplex Decode and Forward Relaying Network with Hardware Impairment over Rician Fading Channel: System Performance Analysis. *Elektronika Ir Elektrotehnika*. 2018, vol. 24, iss. 2, pp. 74–78. DOI: 10.5755/j01.eie.24.2.20639.
- [57] T. N. NGUYEN, N. N. THANG, B. C. NGUYEN, T. M. HOANG, and P. T. TRAN. Intelligent Reflecting Surface Aided Bidirectional Full-Duplex Communication System with Imperfect Self-Interference Cancellation and Hardware Impairments. *IEEE Systems Journal*. 2023, vol. 17, iss. 1, pp. 1352–1362. DOI: 10.1109/JSYST.2022.3167514.
- [58] TAM N.K., D-T. DO, X.N. XINH, T.N. NGUYEN, and H-H. DUY. Wireless Information and Power Transfer for Full-Duplex Relaying Networks: Performance Analysis. *The 2nd International Conference on Advanced Engineering-Theory and Applications (AETA2015)*. 2015, vol. 371, pp. 53–62. DOI: 10.1007/978-3-319-27247-4\_5.
- [59] LE, C.-B., D. T. DO, A. SILVA, W. U. KHAN, W. KHALID, H. YU and N. D. NGUYEN. Joint Design of Improved Spectrum and Energy Efficiency With Backscatter NOMA for IoT. *IEEE Access*, 2022, **10**, 7504–7519. DOI: 10.1109/ACCESS.2021.3139118.
- [60] ZHANG, Q., L. ZHANG, Y.-C. LIANG and P.-Y. KAM. Backscatter-NOMA: A Symbiotic System of Cellular and Internet-of-Things Networks. *IEEE Access*, 2019, **7**, 20000–20013. DOI: 10.1109/ACCESS.2019.2897822.
- [61] JU, J., W. DUAN, Q. SUN, S. GAO and G. ZHANG. Performance Analysis for Cooperative NOMA With Opportunistic Relay Selection. *IEEE Access*, 2019, **7**, 131488–131500. DOI: 10.1109/ACCESS.2019.2940969.